

Space Elevator

Dynamics Reference Manual

**Done by David Lang
in behalf of
Institute for Scientific Research, Inc.
In response to a Funding Contract from NASA, MSFC**

12 April 2006

Contains Section 2 Only

TABLE OF CONTENTS

2.0 GENERAL DYNAMICS	4
2.1 LIBRATION DYNAMICS.....	4
2.1.1 In-Plane Libration.....	4
2.1.2 Out-of-Plane Libration.....	6
2.1.3 Libration Coupling.....	8
2.2 LONGITUDINAL DYNAMICS	10
2.2.1 Longitudinal Bobbing Mass Response	10
2.2.2 Longitudinal Stress Response	14
2.2.2.1 Longitudinal natural modes.....	15
2.2.2.2 Stress wave propagation.....	17
2.3 TRANSVERSE WAVE DYNAMICS	20
2.3.1 In-Plane String Modes	20
2.3.2 Out-of-Plane String Modes	22
2.3.3 Combined In and Out-of-Plane Deflections	24
2.3.4 Transverse Wave Propagation.....	26
2.4 GRAVITY-WELL SIMULATION CONVERGENCE.....	28

INTRODUCTION

This manual is a preliminary work aimed at providing a source of convenient dynamics-related information for those involved with all aspects of space elevator (SE) development and design. For some, this manual may serve as a primer of SE dynamics, for all, it is a source of specific constants, attributes and SE behaviors. This manual is a work in progress as much remains to be addressed as work proceeds on the project. Each section of the manual addresses a special aspect of information pertaining to the SE.

The dynamics attributes have been mostly derived from the time-domain simulation called GTOSS (Generalized Tethered Object Simulation). An outline of GTOSS is included (in Appendices A through D, etc) to allow the user to assess the pertinence of this simulation in providing such results for each aspect of SE dynamics. Related materials re-organized and derived from these studies by the author appear in the papers listed among the references.

General Note: *Some items below should be included for future efforts*

- a. Thermal response*
- b. Climber attitude dynamics*
- c. Ocean wave effects on longitudinal dynamics*
- d. Sun-Moon tidal effects*
- e. Aerodynamic pull-down response*
- f. Breakage debris-footprints*
- g. General pull-down response*

2.0 GENERAL DYNAMICS

2.1 LIBRATION DYNAMICS

The space elevator has two natural modes of oscillation whereby the ribbon, while essentially maintaining a straight line, pendulum's back and forth both in the plane of earth rotation, and normal to the plane of rotation. These are termed "in-plane libration" (east/west motion relative to the vertical), and "out-of-plane libration" (north/south motion relative to the vertical).

For small linear oscillations, the frequencies of these two are:

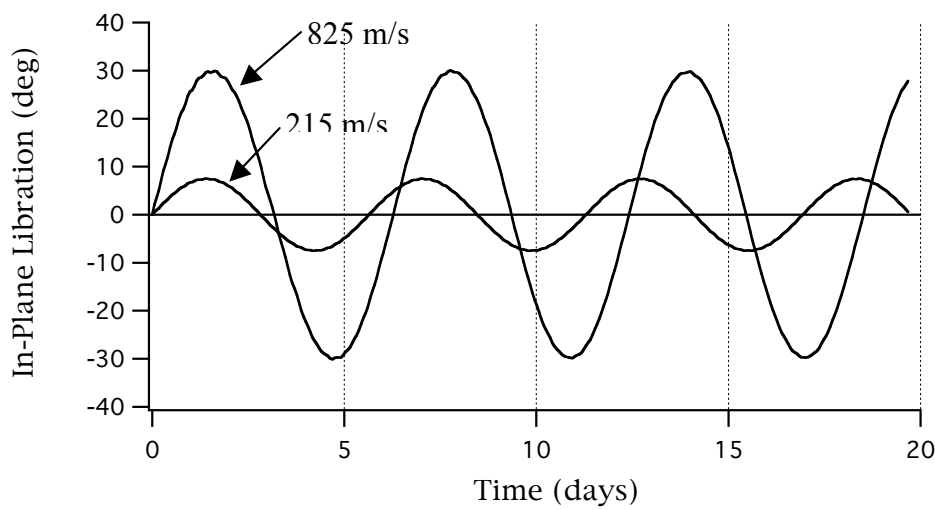
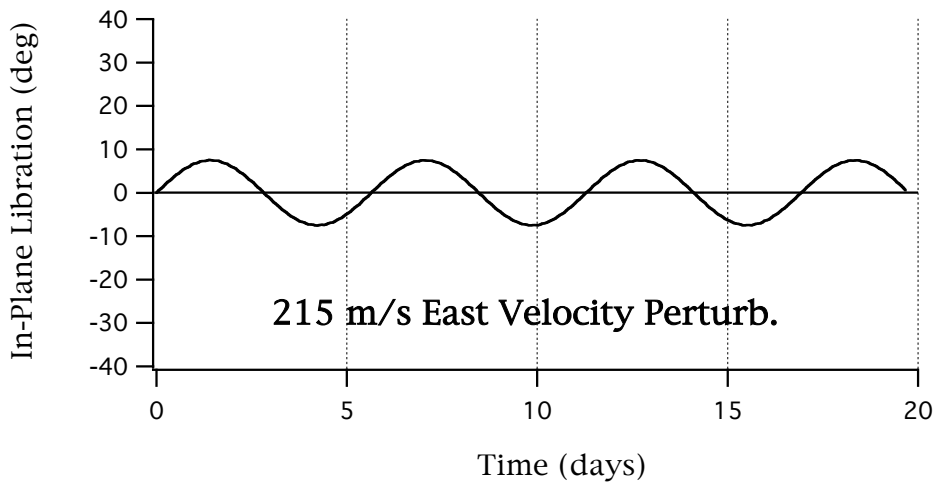
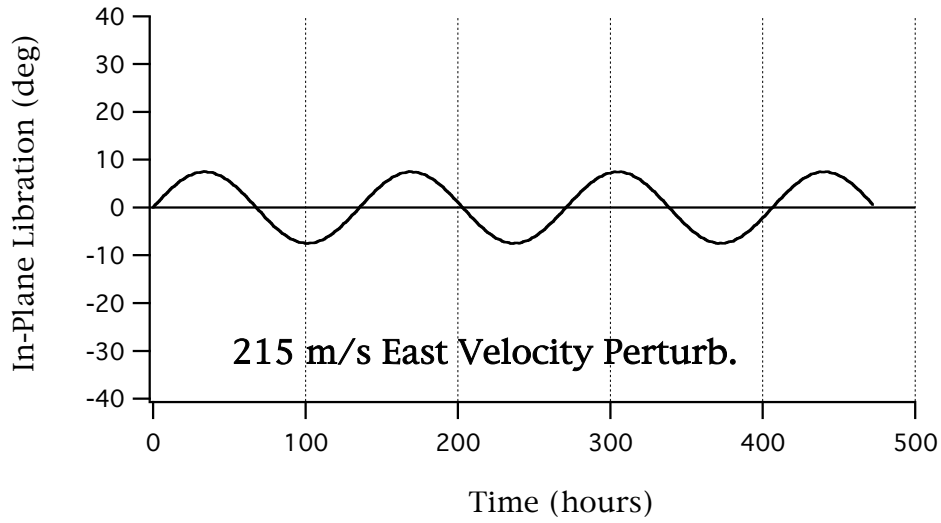
In-Plane (East-West) Libration: 135.6 hrs = 5.65 days (= 488 Ksec)

Out-of-Plane (North-South) Libration: 23.95 hrs = 0.98 days (= 86.2 Ksec)

Note the difference between in and out-of-plane frequencies; this is characteristic of large scale tether dynamics in free earth orbit, and is even more exaggerated in the case of the space elevator. A heuristic way to look at this difference between in and out-of-plane behavior for the space elevator relates to the fact that in-plane libration involves motion *in the direction of the point of constraint* (ribbon anchor), while out-of-plane libration involves motion *normal to the motion of the anchor*. In the case of in-plane motion for example, a velocity perturbation causing libration deflection eastward also experiences the anchor point progressing eastward under it, thus slowing overall eastward migration of the ribbon, producing a longer time period to reach a given libration angle. Such an intuitive explanation may or may not be accurate, but what is accurate are the governing equations of motion, in which this effect manifests itself precisely in the equations as certain relative-motion coupling terms, for which an intuitive explanation, while possibly satisfying, is not required to produce the effect.

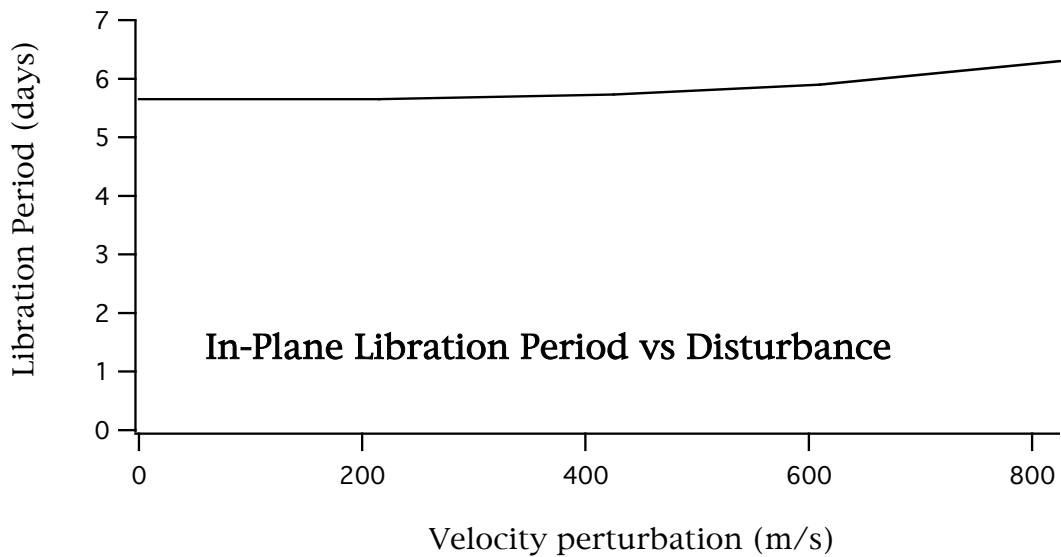
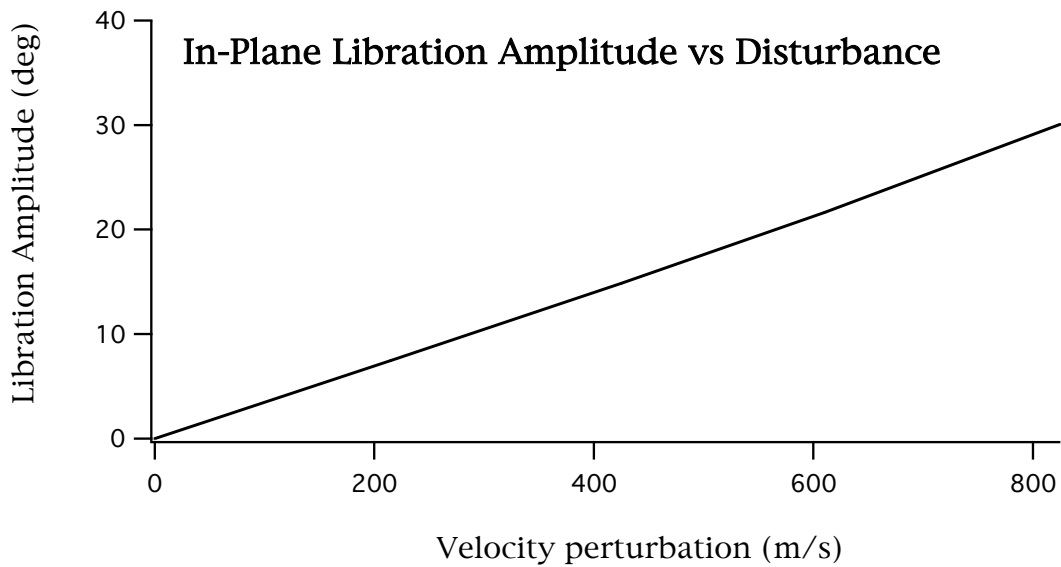
2.1.1 In-Plane Libration

For a perfectly stable elevator, the ballast has a velocity relative to the earth anchor point of 7292 m/s in-plane (= 23,900 ft/sec = 16,300 mph), and *zero velocity* out-of-plane. All the graphs of libration response below were produced by introducing various "speed perturbations" to the ballast; in the case of in-plane perturbations, these ranged up to about 10% over-speed (relative to the nominal stable in-plane relative velocity).



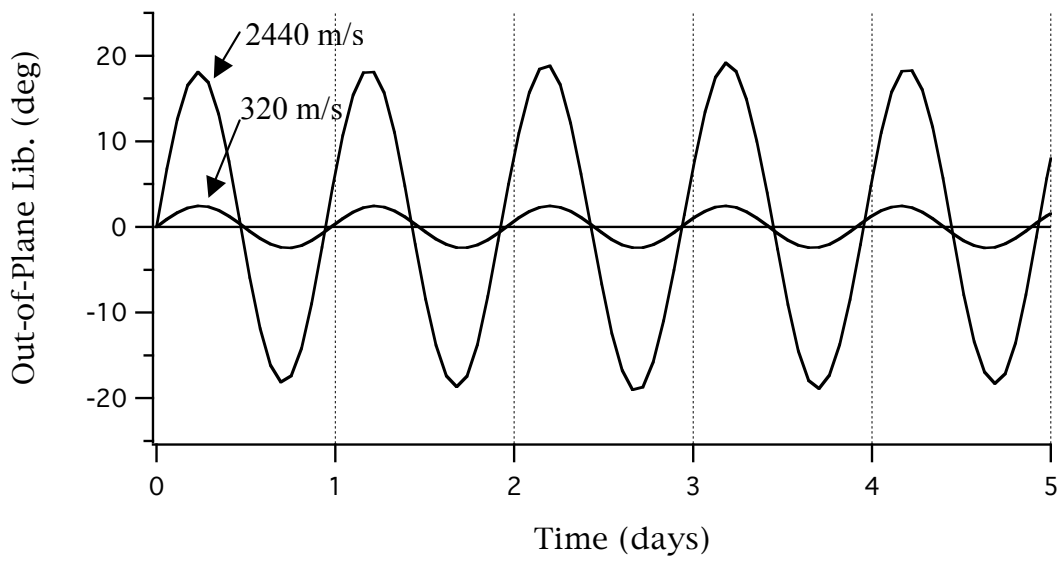
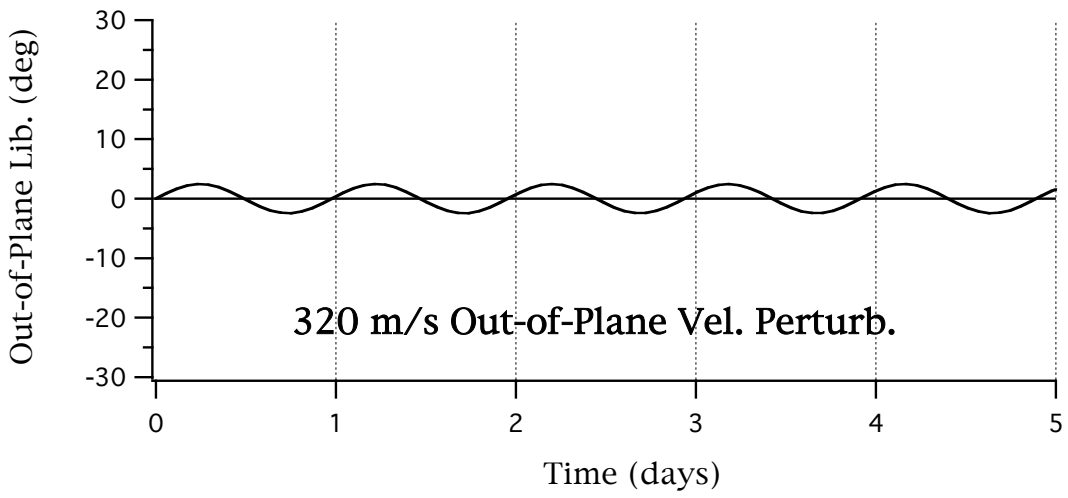
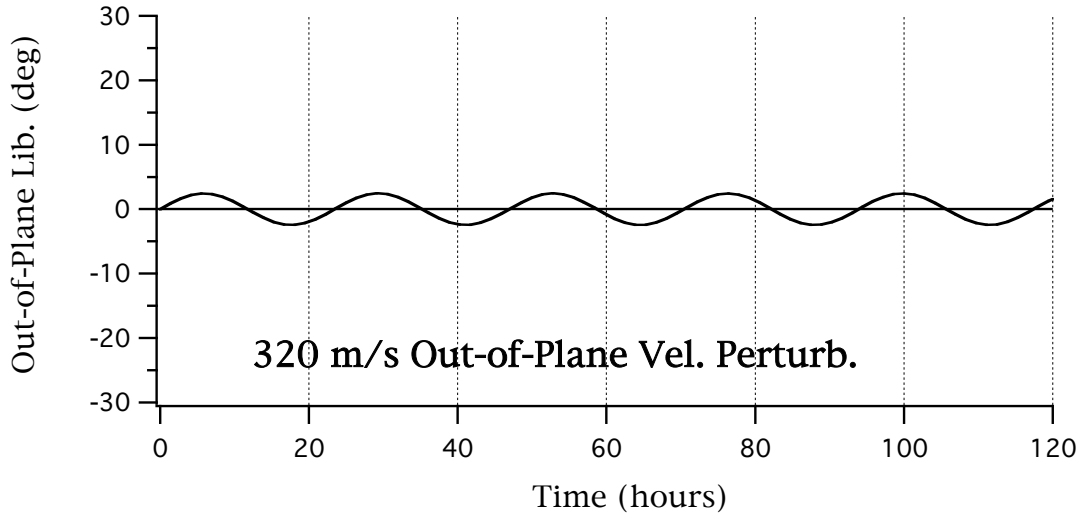
The graph above shows how both amplitude and period increase as in-plane libration perturbation increases.

Below is shown the peak amplitude and period of in-plane libration as a function of perturbation velocity.



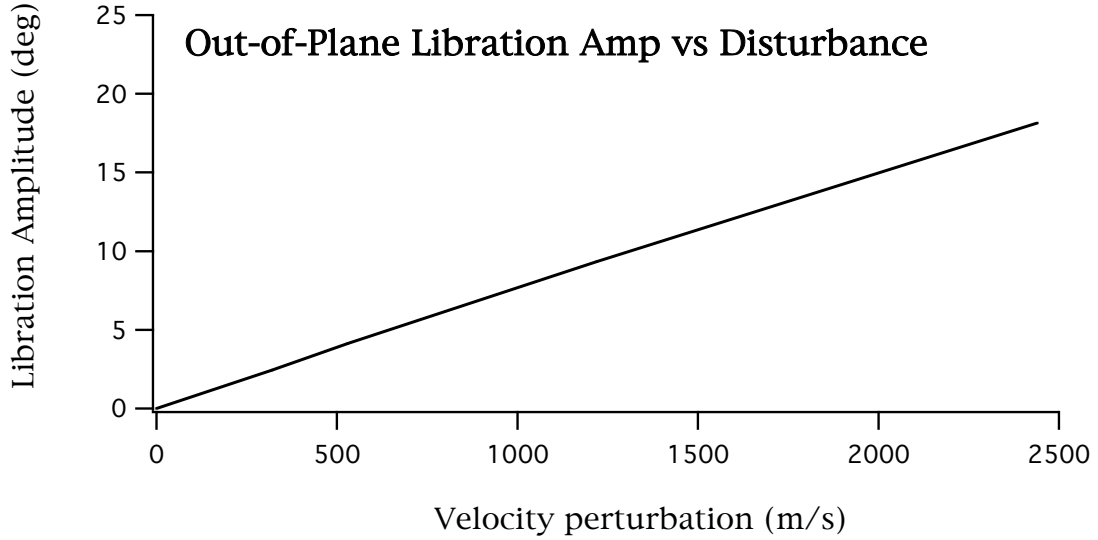
2.1.2 Out-of-Plane Libration

For a perfectly stable elevator, the ballast has an out-of-plane velocity relative to the earth anchor point of *zero*. All the graphs of out-of-plane libration response below were produced by introducing various “speed perturbations” to the ballast; in the case of out-of-plane perturbations, these ranged up to almost 5000 m/s.



The graph above shows that unlike in-plane libration, out-of-plane libration period is very insensitive to libration amplitude.

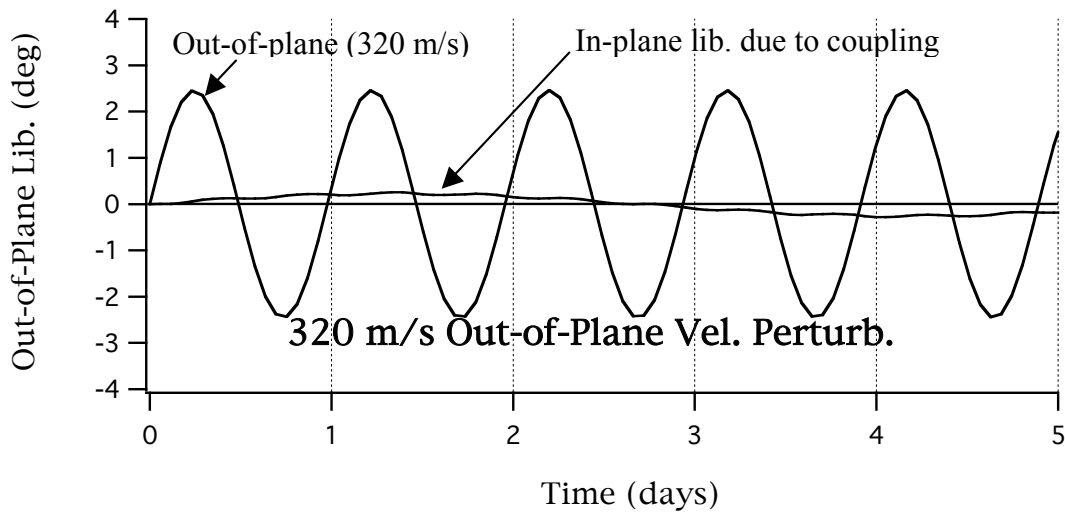
The graph below shows how out-of-plane libration amplitude varies as a function of velocity perturbation.

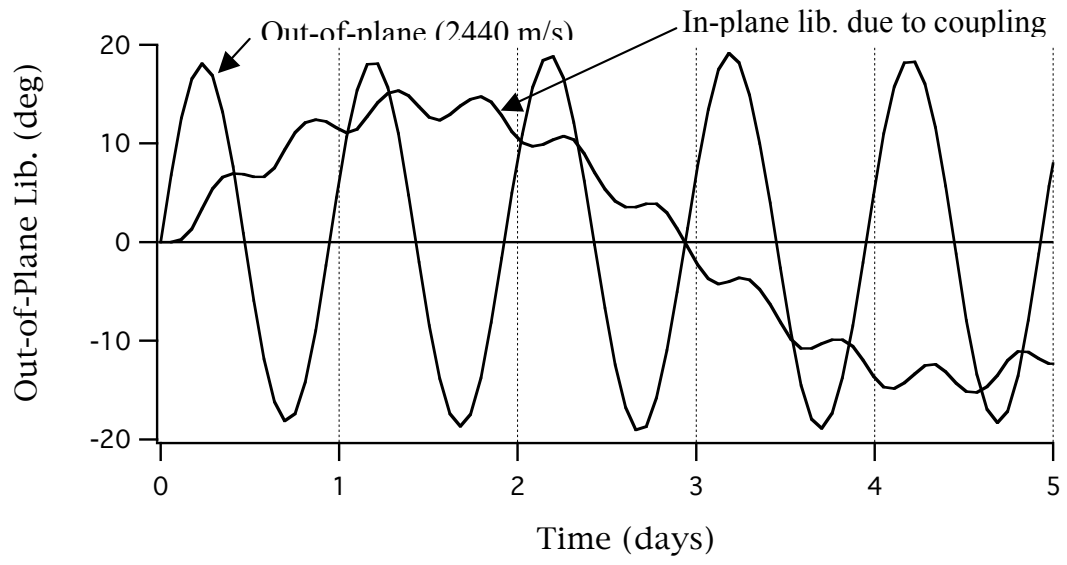


2.1.3 Libration Coupling

Point of Interest: Coupling of out-of-plane libration into in-plane libration can occur due to the effects of Coriolis acceleration and in/out of plane velocity resolution. At low amplitudes this is very mild; at large amplitudes it can be significant.

The graphs below illustrate coupling of out-of-plane libration into in-plane libration for two different levels of out-of-plane libration.



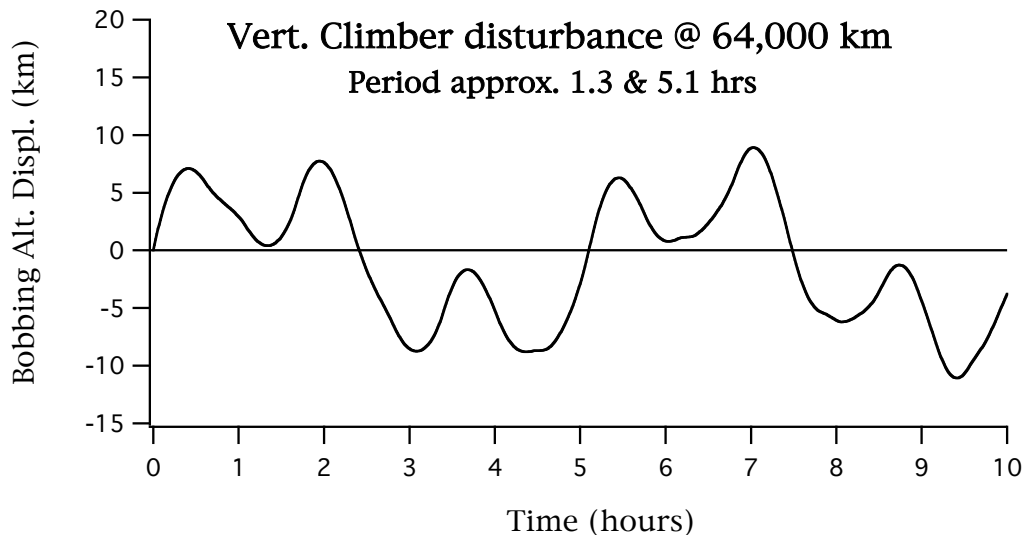
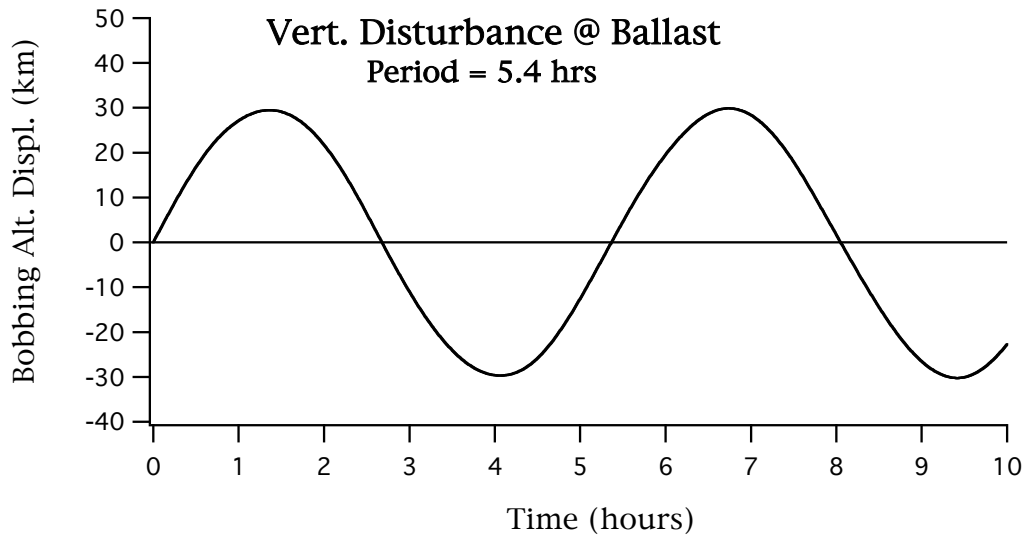


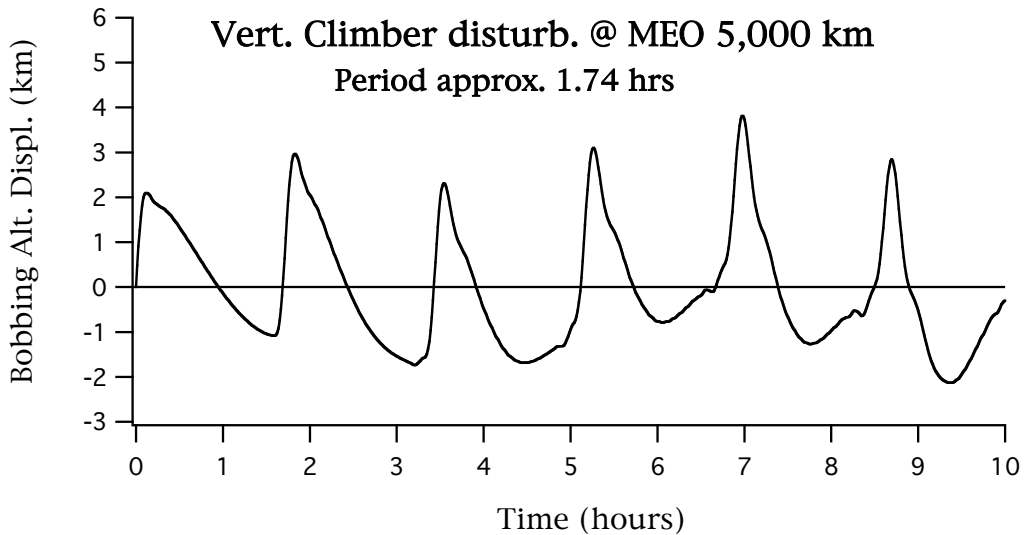
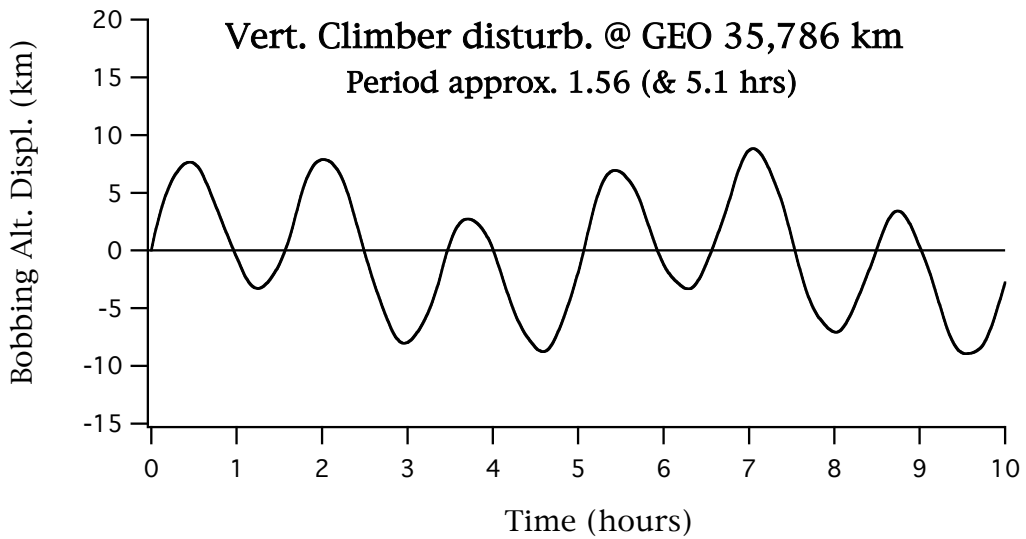
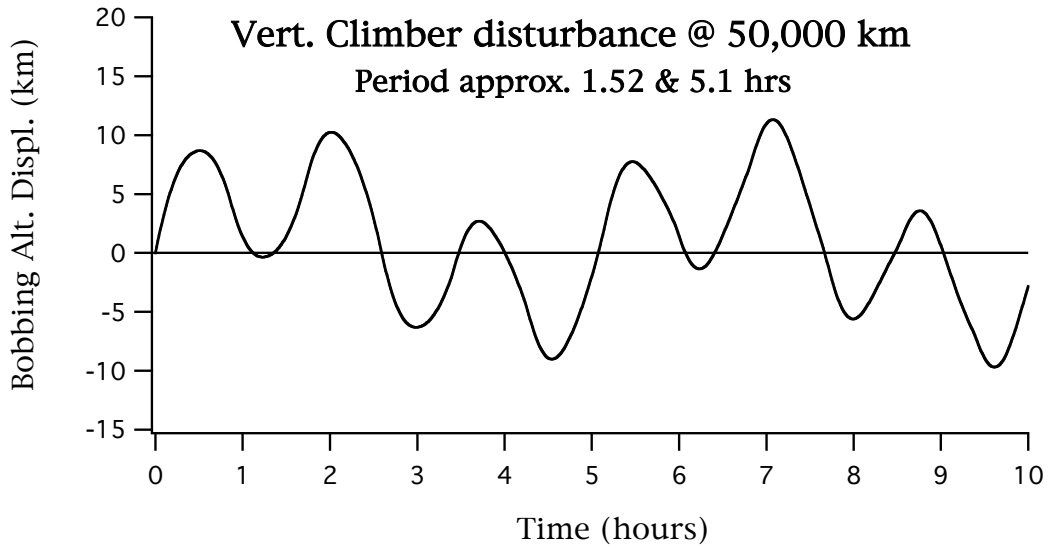
2.2 LONGITUDINAL DYNAMICS

This section provides information about the various types of dynamics responses characteristic of the longitudinal axis of a space elevator

2.2.1 Longitudinal Bobbing Mass Response

Longitudinal bobbing response of the space elevator manifests different attributes at different altitudes. Longitudinal bobbing was initiated by imparting a 10 m/s positive altitude rate to an otherwise stable elevator configuration. The overview presented here starts with an unoccupied elevator with just a Ballast mass to which an altitude rate is imparted; all other cases have a climber attached in a stable configuration prior to being given a positive altitude rate, thus these results also are equivalent to the sudden arrest of a climber traveling upward at 10 m/s. The results below present disturbances at varying locations of interest along the ribbon.

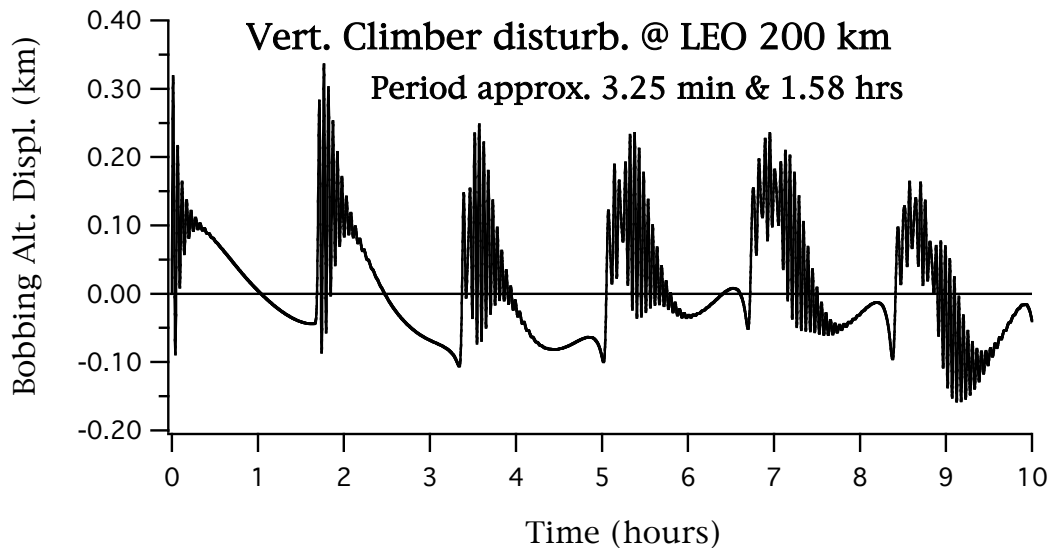




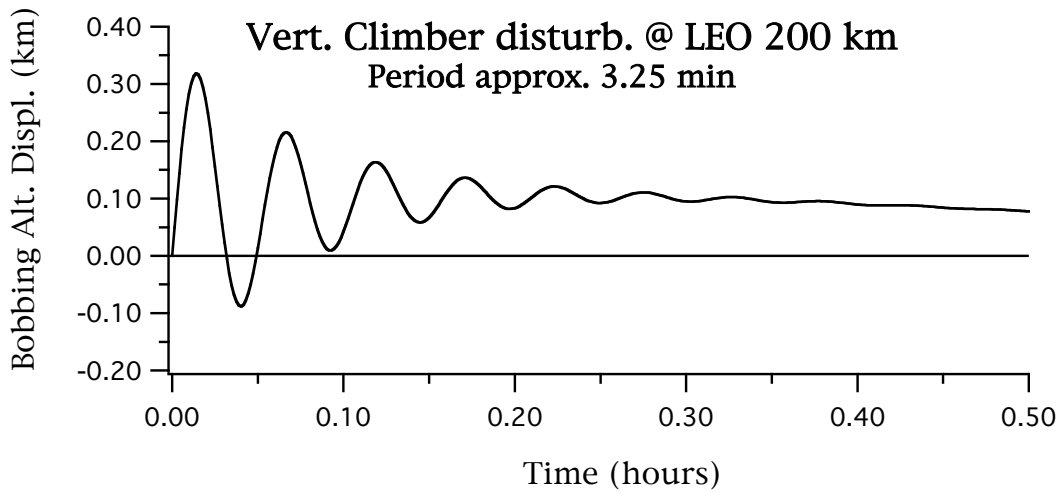
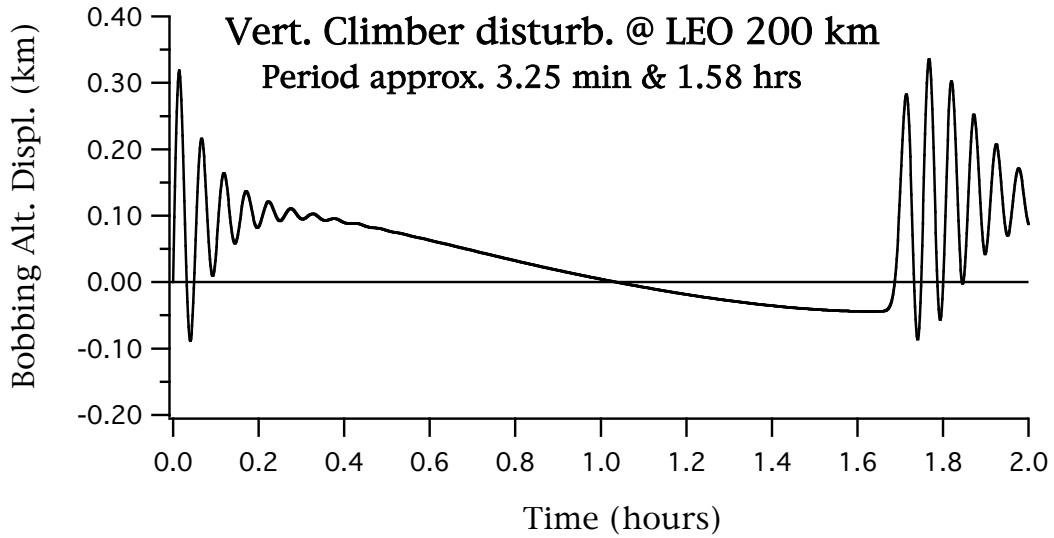
The response at MEO (above) is starting to manifest the effects of the growing differences in the effective spring rates of the ribbon above and below the climber as the distance between the climber and ground diminishes.

Point of Interest: Only the case of the unoccupied elevator, with the ballast given a longitudinal disturbance, produces what is essentially simple harmonic spring mass response; all other manifestations of longitudinal response are of more a complex vibratory motion. This can be attributed to the fact that the climber might be simplistically thought of a mass attached to two springs of different spring rates (the upper and lower ribbons), each of which is under a different pre-load (due to the presence of the climber itself in the gravity field); and this combined with the significant mass/elasticity of the ribbon itself.

The longitudinal bobbing shown below for the case of a climber at LEO (200 km) appears to present two extremely diverse frequency components, one of 3.25 minute period, and the other, almost 2 hours. The high frequency is due to the interaction of the climber with the high spring rate of the relatively short ribbon section (200 km) interposed between the ground and the climber (this compared to the almost 100,000 km long spring between the ballast). This interaction is shown to be larger damped out by 15 minutes. However, the stress perturbation signature experienced by the ribbon was broadcast in both directions along the ribbon. That headed towards the ground reappears in such a short time (round trip to ground and back being about 7 sec) that it is essentially being seen as a part of the initial response; that headed towards the climber however, has a 1.58 hour round trip facing it. Thus, well over an hour later reappears at the climber to again perturb it. The ensuing re-appearances of this rogue-disturbance become increasing complex by interaction with its own reflections, the climber mass, and the mass of the ribbon itself.



The two graphs below depict these characteristic wave responses in finer detail.



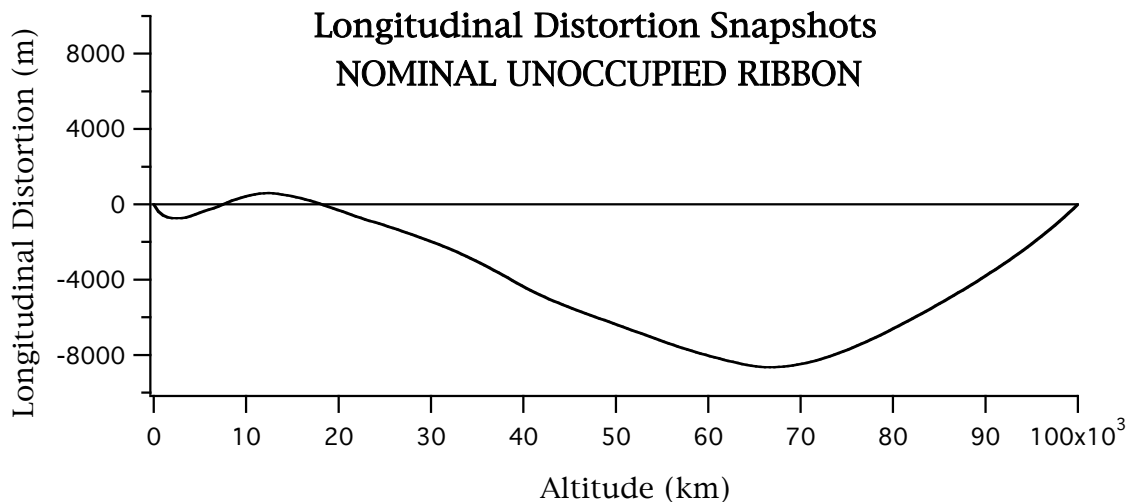
Point of Interest: The longitudinal response shown for the case of the climber at LEO and MEO would be essentially duplicated if the climber were to be suddenly arrested within 200 km of the ballast mass. Such complexity of motion is already beginning to manifest itself in the case (above) of the longitudinal disturbance at 64,000 km.

2.2.2 Longitudinal Stress Response

The case (above) of climber longitudinal bobbing at LEO altitude presented a situation where the propagation and reflection of stress waves along the ribbon was both of sufficiently short and long duration (compared to the original disturbance), that there was both a *coalescence* and a *disassociation* of the reflections with the original disturbance. Two phenomena manifest themselves in longitudinal dynamics, (a). propagation of transient stress disturbances, and, (b) coherent propagations that manifest themselves as longitudinal natural elastic (ie. normal) modes of the ribbon mass-elasticity continuum. As distinguished from random stress disturbance propagation, longitudinal natural modes are characterized by all the particles of the ribbon moving at the same frequency (ie. in phase, but not necessarily in the same direction).

Point of Interest: the term “Longitudinal Distortion” refers to the amount that a ribbon particle is displaced axially from the position it would occupy were the ribbon in a quiescent state under no external forces. So, by necessity, a perfectly stable elevator would exhibit a **non-zero** longitudinal distortion, this being required to equilibrate the ribbon particles via internal ribbon stress against the external gravity-centripetal field.

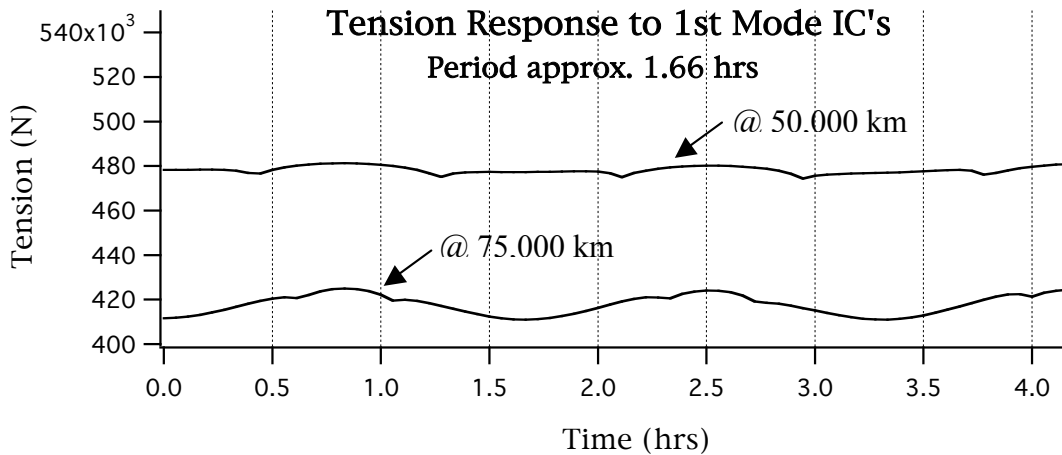
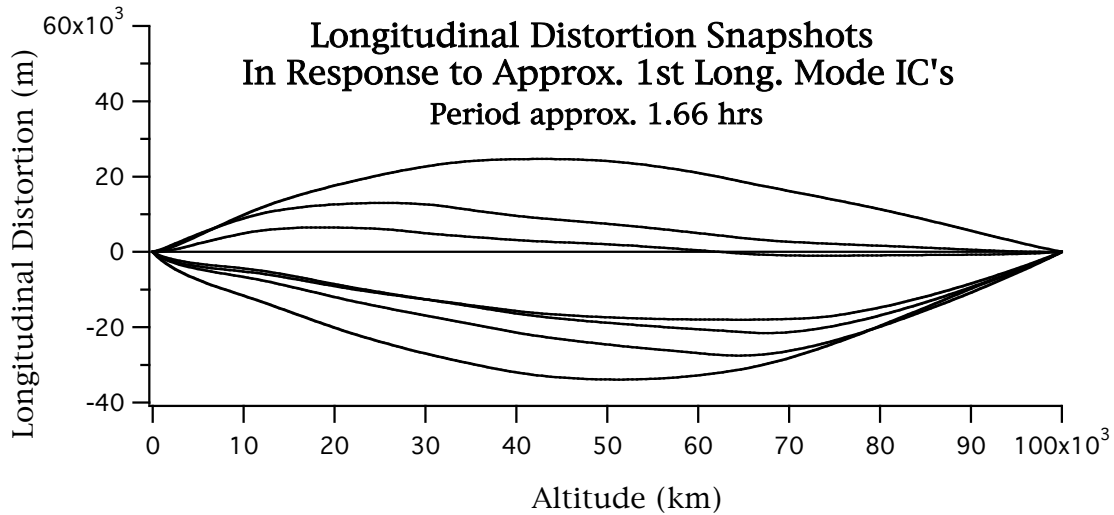
Shown below is the Longitudinal Distortion inherent in a stable, unoccupied elevator ribbon. This is a longitudinally un-symmetrical distribution, unlike the distortion distributions of classical natural longitudinal modes. Note that in order to invoke strong natural “longitudinal modal responses”, initial peak displacements for the modal initialization must significantly over-shadow this initial strain state; thus, for the natural mode initializations shown later, the peak amplitudes are 100,000 m (compared to 8,000 m for the stable elevator configuration shown below).

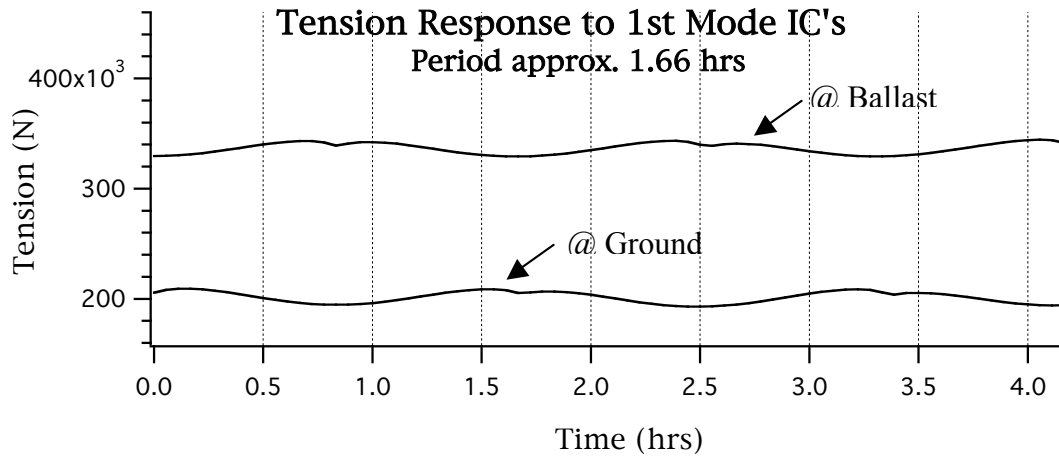


2.2.2.1 Longitudinal natural modes

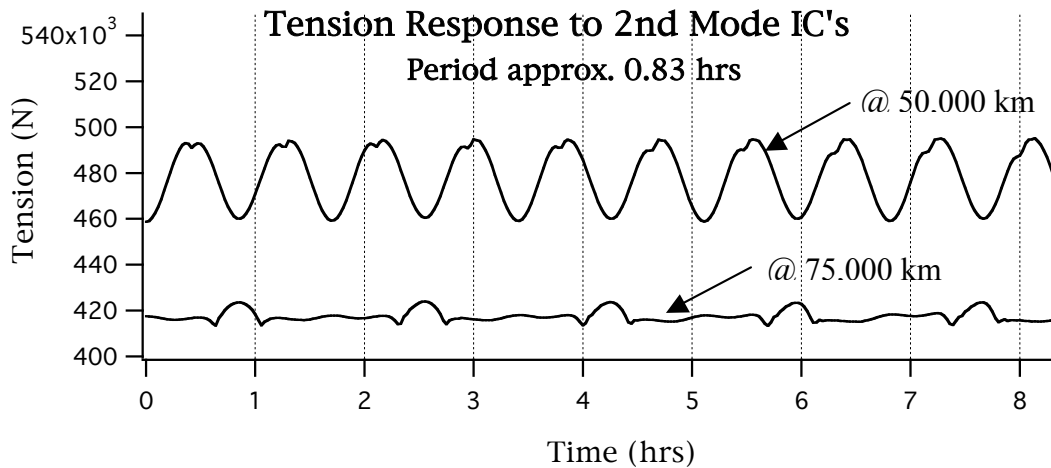
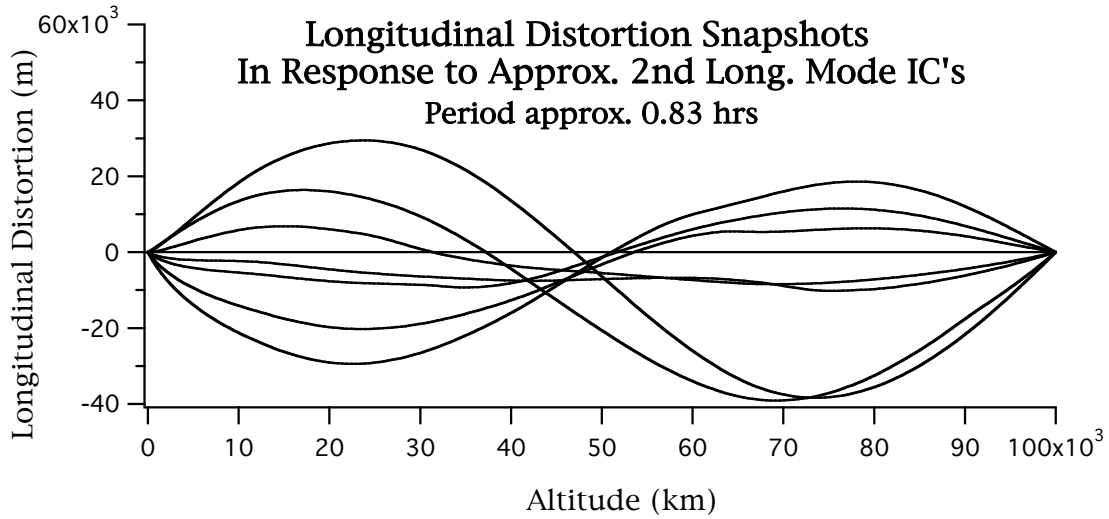
Examples of response for the first two natural modes are shown below. Note that these modes do not exhibit pristine behavior due to the fact that longitudinal initialization is attempted in the form of sinusoidal shapes applied against the longitudinal distortion extant in the elevator ribbon due to its stabilized state in the presence of the combined gravity-centripetal field. Such anomalies manifest themselves in the form of “modal displacement shapes” and time histories of stress-related parameters (like tension) that do not exhibit pristine sinusoidal shapes. Nodal points (that classically exhibit null response) will correspondingly be ill defined.

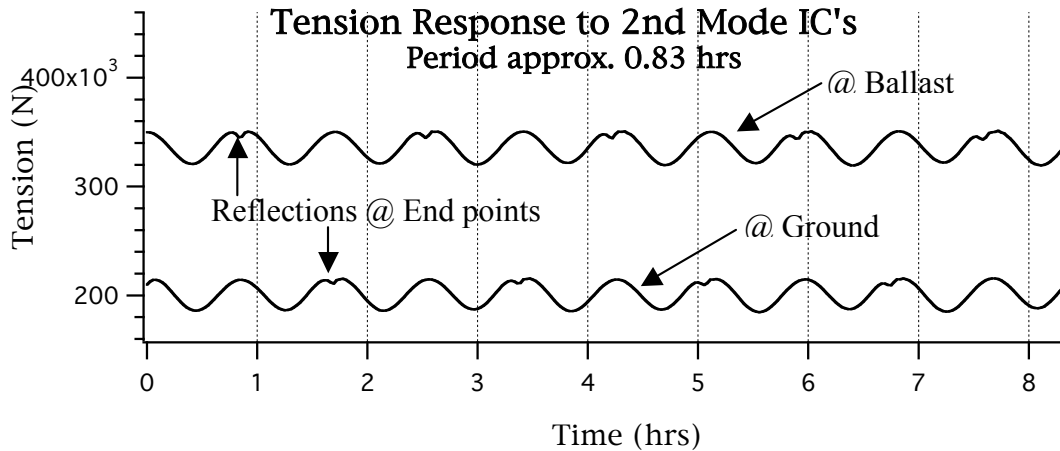
Below are results for ribbon response given an initial state corresponding to the first longitudinal natural mode.





Below are results for ribbon response given an initial state corresponding to the first longitudinal natural mode.





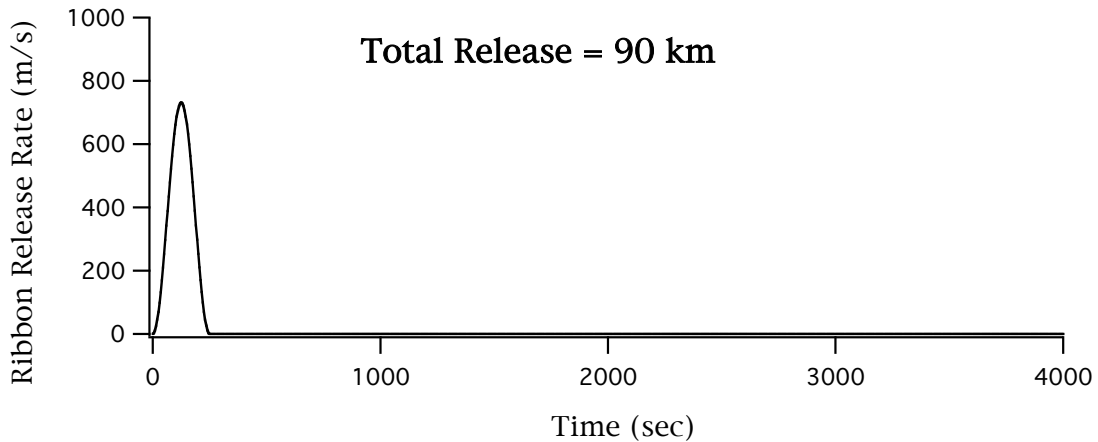
Point of Interest: In the above graph, notice the stress disturbance that appears (at the tension peaks) and alternates between for the ballast and the anchor. This was introduced due to a “Classical longitudinal 2nd mode initial condition” being superimposed onto the initial asymmetric strain distribution of the stabilized ribbon. The disturbance, effectively originating near the ground, is seen to impact and reflect off the ballast in a little less than an hour (the one-way transit time for a ribbon stress wave disturbance), then impact the anchor point about an hour later, thereafter, alternating back and forth from top to bottom. Notice also that this same disturbance is manifesting itself at the mid-point (previous graph) on a more or less hourly basis; this is because the mid point is about a 25 min transit time from either end, and catches the disturbance coming and going).

2.2.2.2 Stress wave propagation

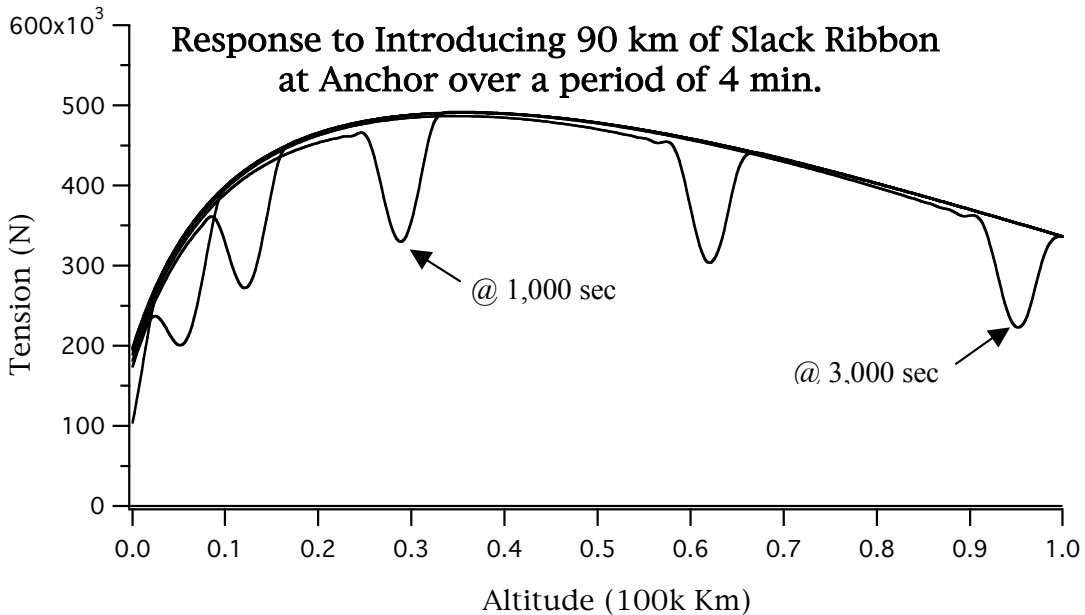
Stress wave propagation is a phenomena related to only two ribbon material properties; modulus of elasticity, and density. It can be thought of as the “speed of sound” for the medium. A steel rod if hit on one end will transmit that impact (which could actually be audible) along the length of the rod at the inherent speed of stress wave propagation. This speed, corresponding to solids, is significantly different from that of air (usually an order of magnitude greater). The graph just above (last graph in the previous section) exhibits this phenomenon.

Stress disturbance can be associated with any phenomenon that creates a strain (stress) gradient. Longitudinal natural modes correspond to a form of stress wave propagation, although in that case it is *coherent*; conventionally, stress wave propagation refers to disturbances of a non-coherent nature. For the further demonstration of stress propagation in the space elevator ribbon, this section will employ the introduction of a stress gradient by way of releasing a portion of slack into the domain of the ribbon.

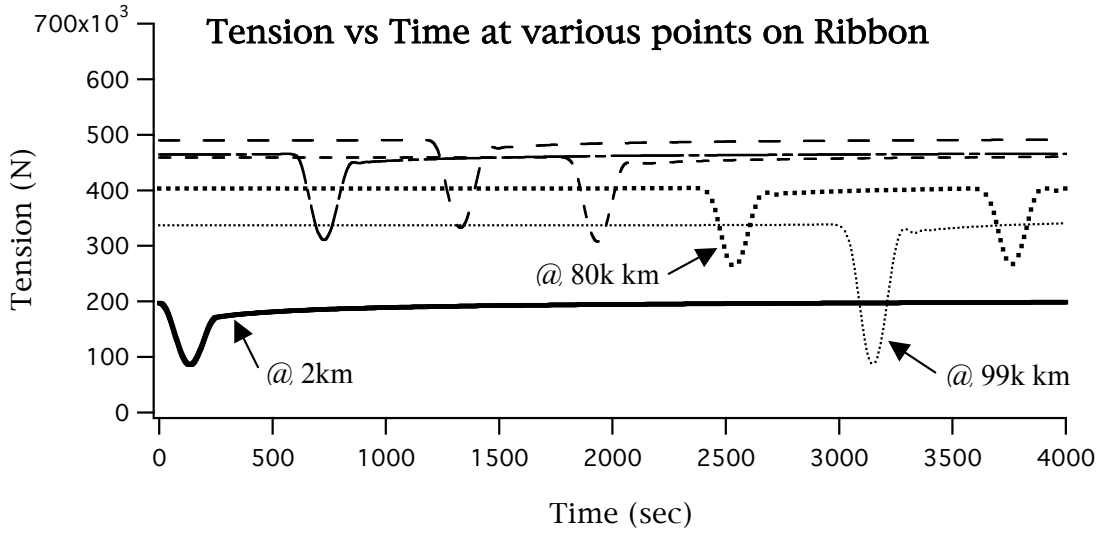
Specifically, 90 km of slack ribbon are introduced into the ribbon at the anchor; this creates a large low tension disturbance that then propagates up the ribbon towards the ballast. The release profile in time is shown below.



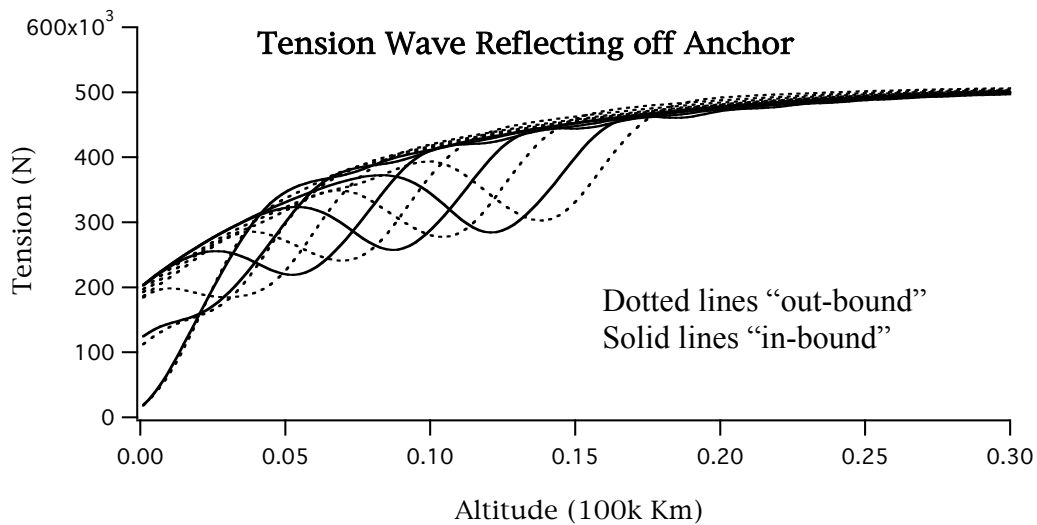
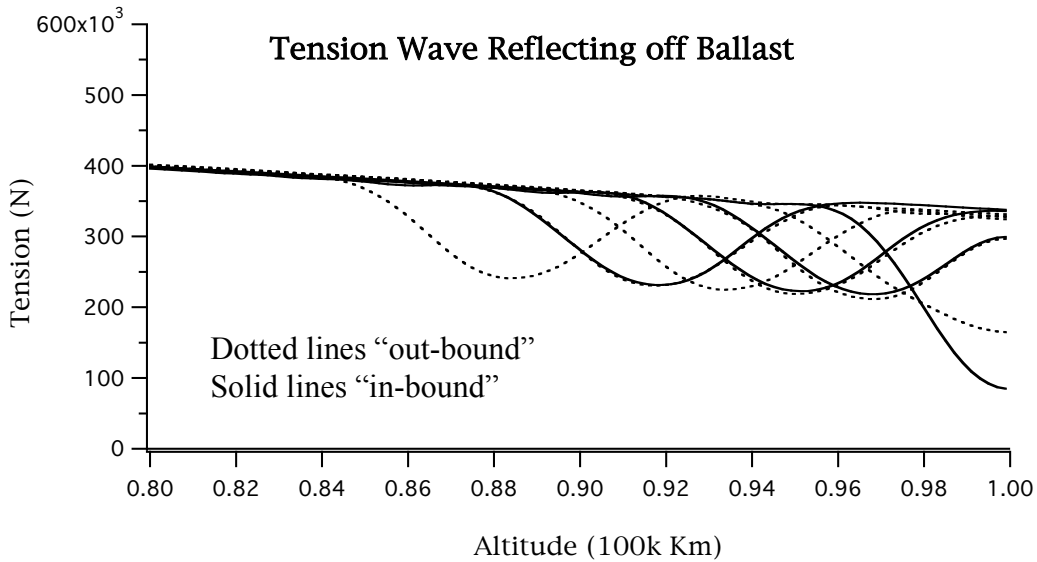
Below is the a series of snapshots of the resulting tension response as it progresses up the ribbon. The snapshot at 3,000 sec shows the stress wave poised to impact the ballast.



The graph below shows the time history of tension at various altitudes along the ribbon, starting at 2 km, then progressing up through 20k, 40k, 60k, 80k, 99k kilometers. Note that the tension disturbances are uniformly distributed in time (due to the uniform sample distances along the ribbon and the constant transmission speed). The stress wave shown at the 99k km position is poised to reflect off of the ballast, a fact that indeed manifest itself in the tension history at the 80k km point, for which is shown two disturbances, symmetrical-in-time about the reflection time (first disturbance at about 2600 sec, then the reflected disturbance coming back across the 80k km point at about 3800 sec).



The graphs below show the tension wave reflecting off of the Ballast, then the Anchor.



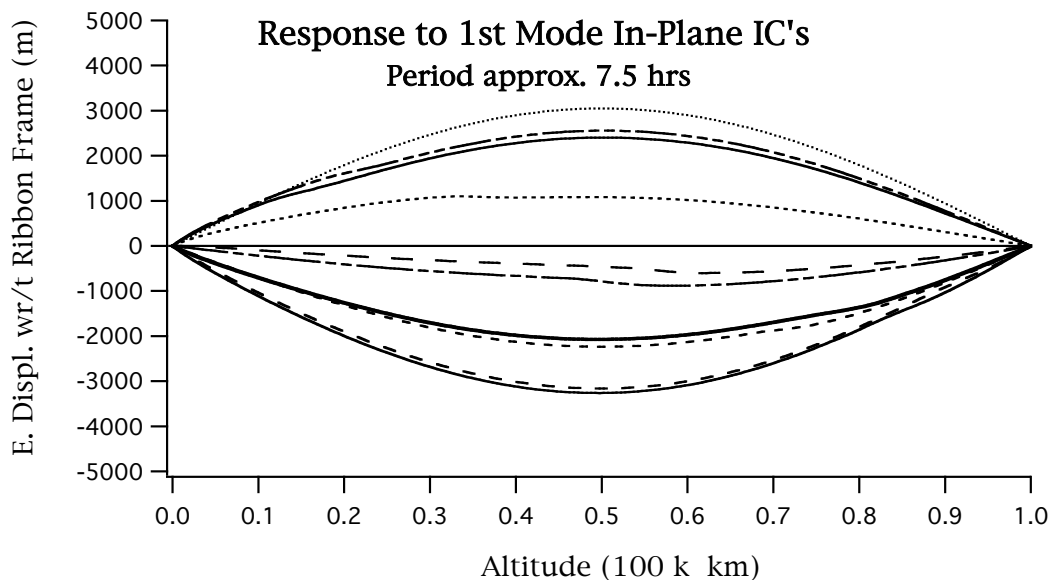
2.3 TRANSVERSE WAVE DYNAMICS

Classical solutions for the one-dimensional string equation require an assumption of uniform and constant string tension along with a constant lineal mass density. Under these conditions, closed form solutions yield the familiar sinusoids for natural (normal) modes of vibration. It would appear that the space elevator ribbon would significantly violate such assumptions since its tension and mass density vary considerably over length. However, the constant-stress space elevator ribbon design, by virtue of its criteria to produce uniform stress distribution under (unoccupied) non-linear gravity and centripetal loading, fortuitously creates approximate lineal properties distribution, which, when combined with ribbon tension variation, can render the coefficient of the one-dimensional classical string equation nearly constant, thus meeting requirements for the classical closed-form solutions in response to initial conditions. Thus the unoccupied ribbon enjoys an approximation the same classical normal modes of vibration as a simple string. Such is born out in the GTOSS simulation of the ribbon in which all these non-linear properties and other effects are combined. Of course if the elevator is occupied by a climber, or subject to disturbances, then resulting modes of vibration may not follow those predicted by classical string equation solutions and response may manifest non-linear attributes that may not be replicable under classical linear analyses.

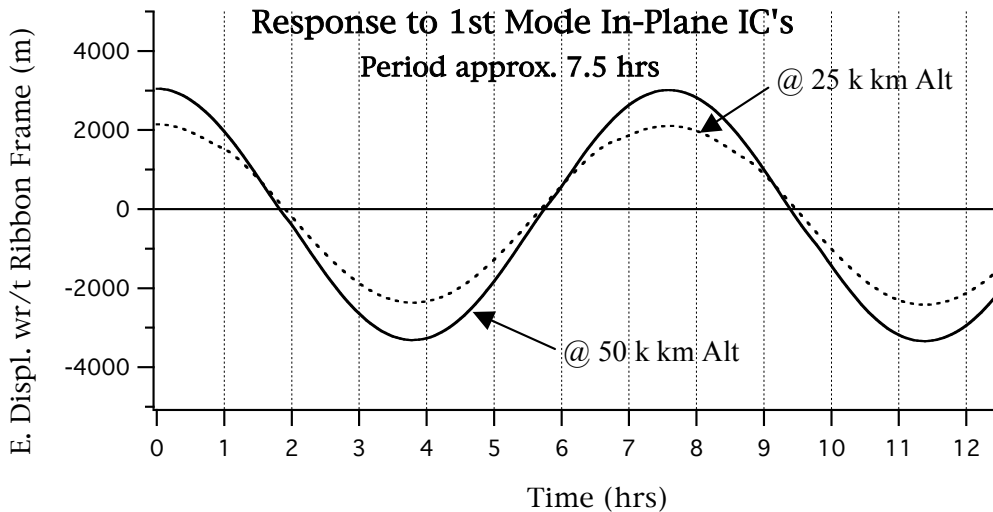
2.3.1 In-Plane String Modes

This section shows response to initializing the ribbon with 1st and 2nd natural mode conditions corresponding to a string fixed at both ends. This is not exactly the conditions presented by the space elevator since the ballast is free to move in libration. Thus the resulting motion will deviate somewhat from classical string response.

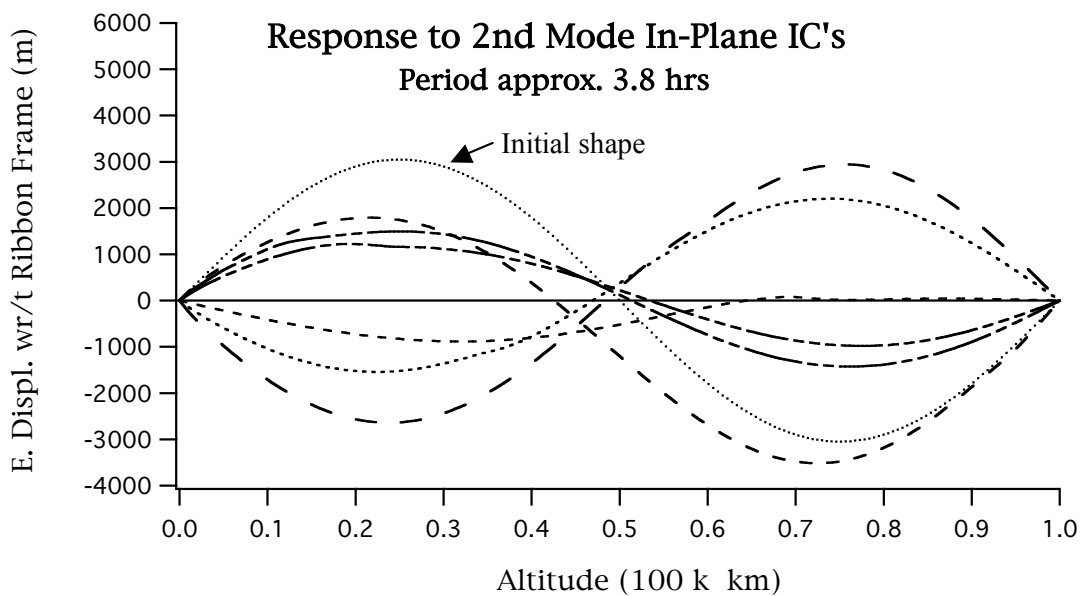
The graph below is a series of in-plane deflection snapshots taken at various times during the 12 hours of simulated time. These are deflections relative to a frame between the anchor and ballast, thus gross pendulus ribbon libration will not be evident.



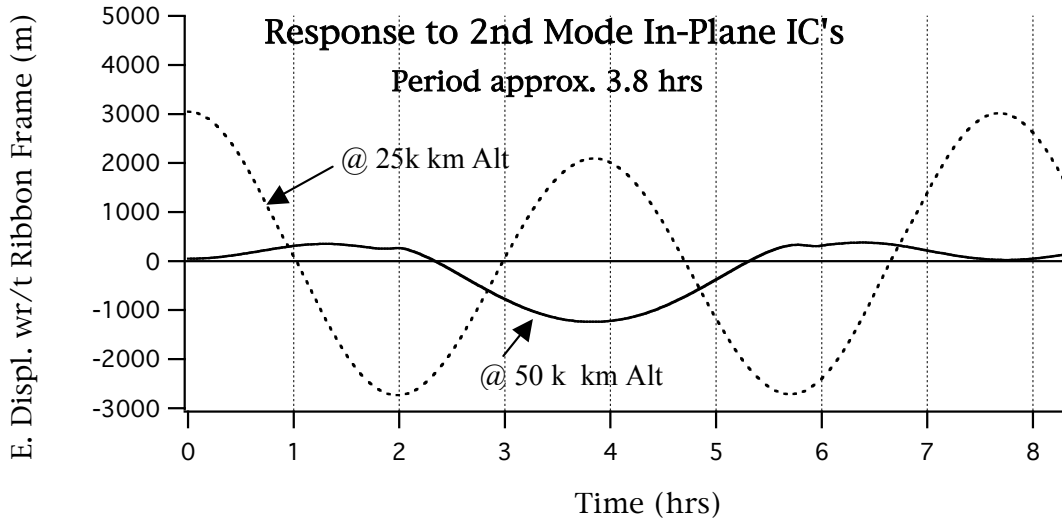
The graph below shows time histories of response (corresponding to the graph above) at the quarter-, and mid-point of the ribbon.



The graph below presents deflection snapshots (similar to above), except these are for the 2nd string mode. Note that initializing the ribbon to a classical 2nd natural mode does not yield as clean a modal response as did the 1st natural mode. The “fine dotted” line is the initial deflection shape; resulting motion exhibits distortion. It might be concluded that the higher the mode number, the more the response will deviate from classical modal response.

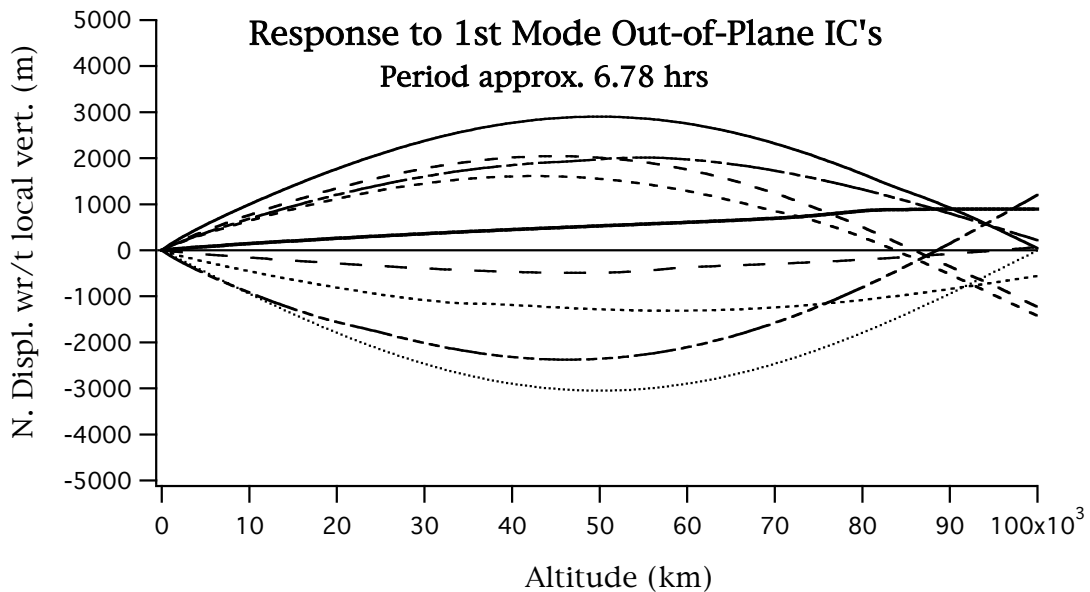


The graph below shows response time histories at the ribbon quarter- and mid-point. This illustrates another view of how resulting response deviates from classical modal response.

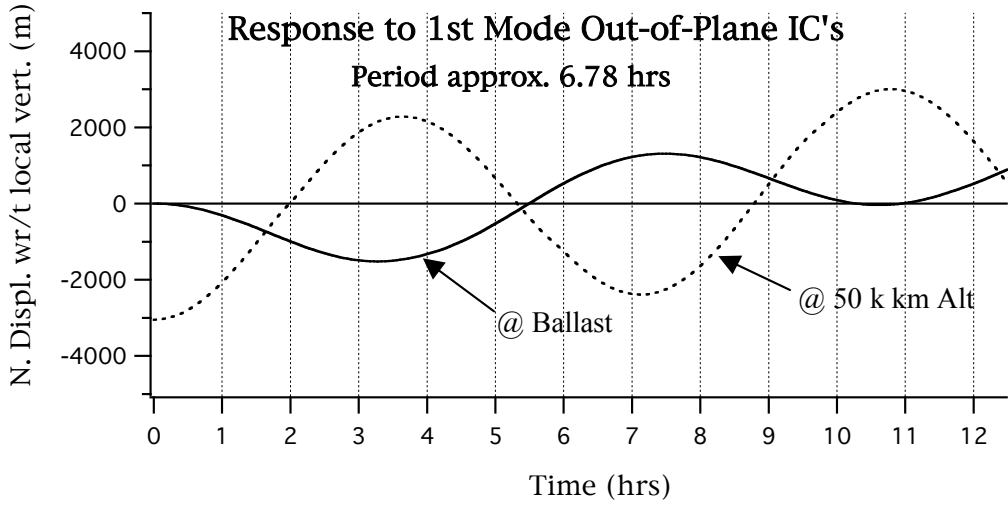


2.3.2 Out-of-Plane String Modes

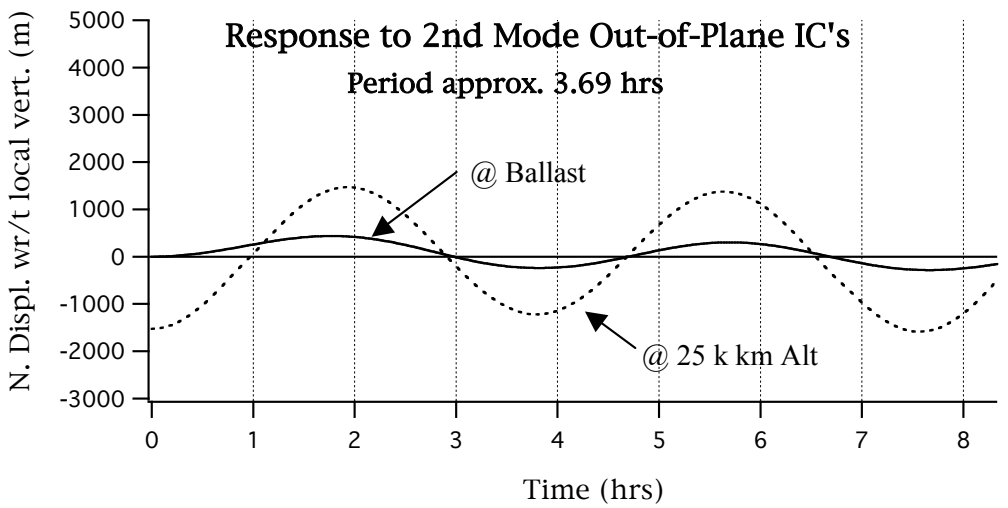
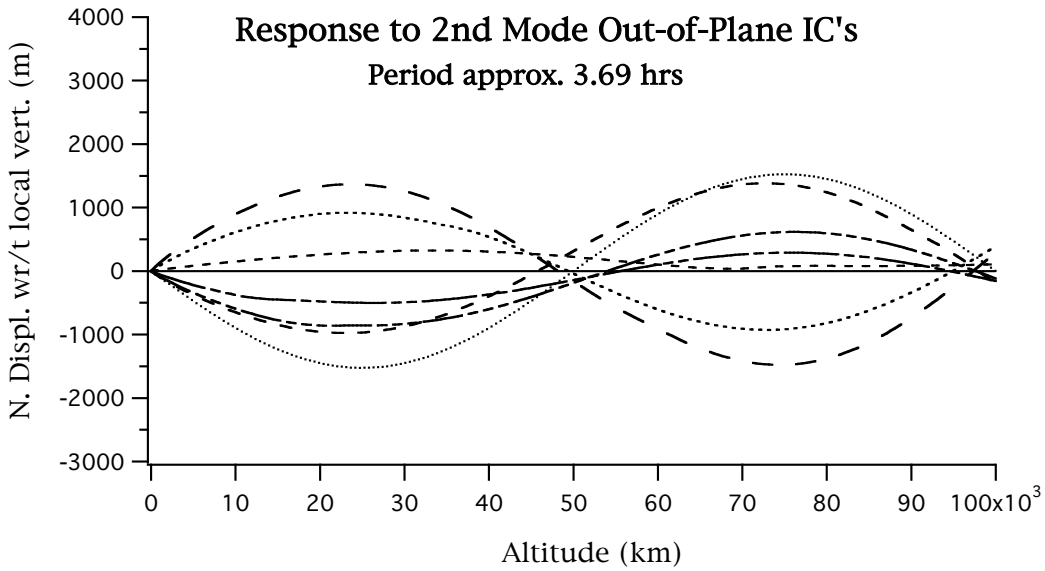
The results below are identical to those of Section 2.3.1, except pertain to Out-of-Plane natural modes. The deflections in these graphs are relative to a vertical passing through the anchor point, thus they can characterize any gross ballast libration component in the response. The libration evident below has resulted from the fact that the modal initial conditions do not the actual *fixed-free* boundary-conditions of the ribbon, but rather correspond to classical *fixed-fixed* boundary conditions.



Note in the graphs below that a component of out-of-plane libration has also been induced due to un-balanced out-of-plane modal initial conditions.



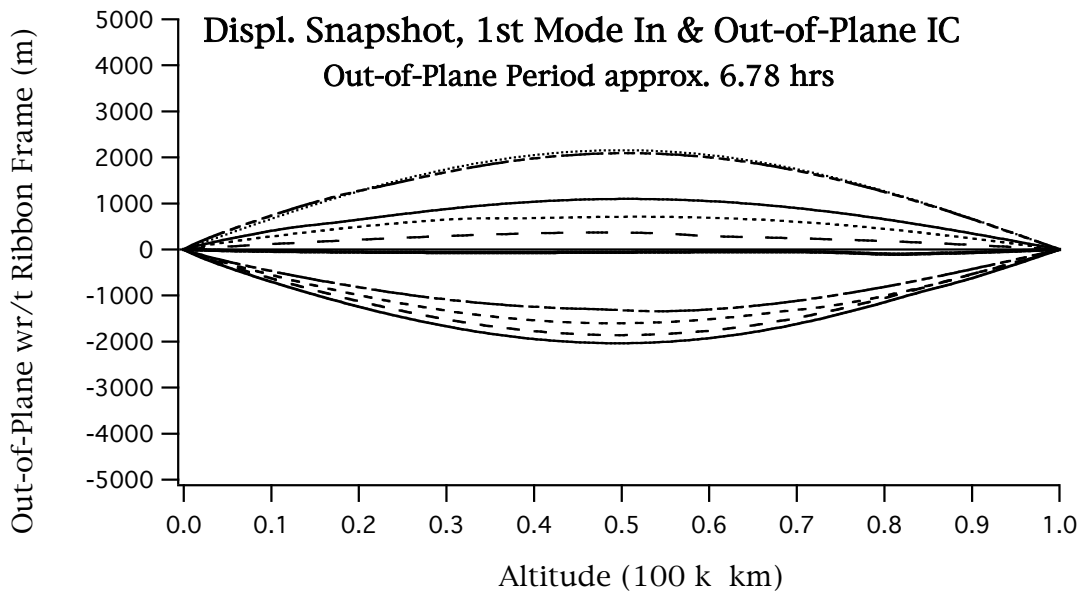
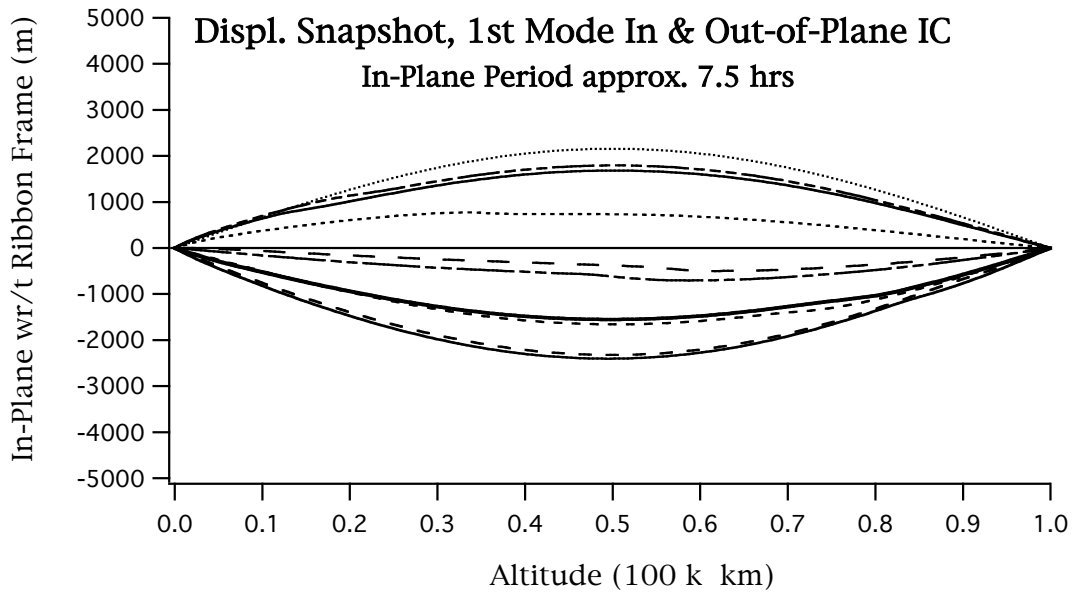
Below are 2nd mode Out-of-Plane response graphs similar to above.



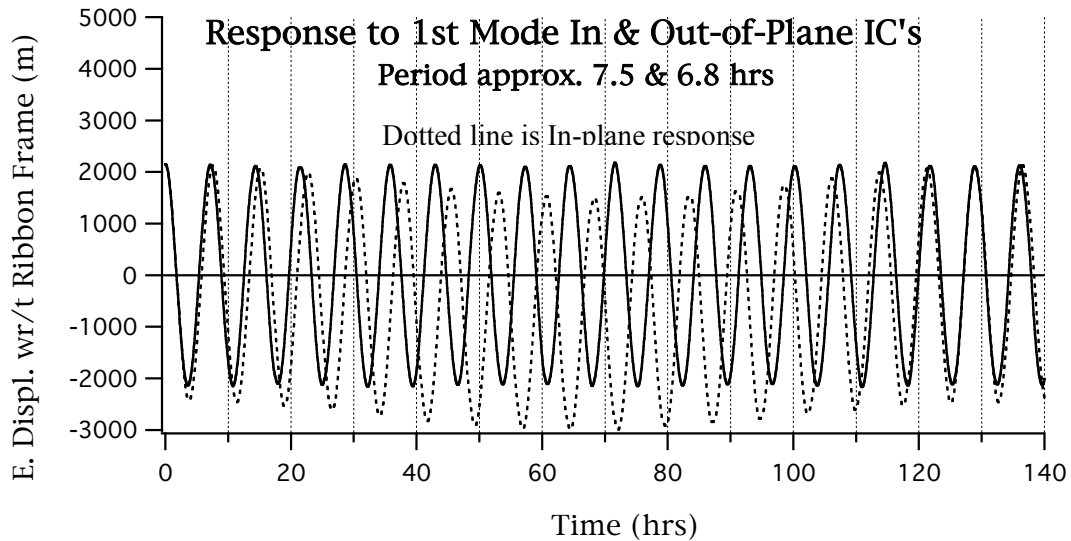
2.3.3 Combined In and Out-of-Plane Deflections

Theoretically, no coupling occurs between normal modes of vibration. Since the constitution of the elevator deviates somewhat from the classical conditions, it is possible that interactions might take place between planes of vibration. This section explores such possible interaction if both in- and out- of-plane modes are excited. In the examples below, the 1st string mode (only) was excited in both planes simultaneously.

The two graphs below show snapshots at various times of the deflection shapes relative to the line between the anchor and the ballast (referred to as the Ribbon frame).

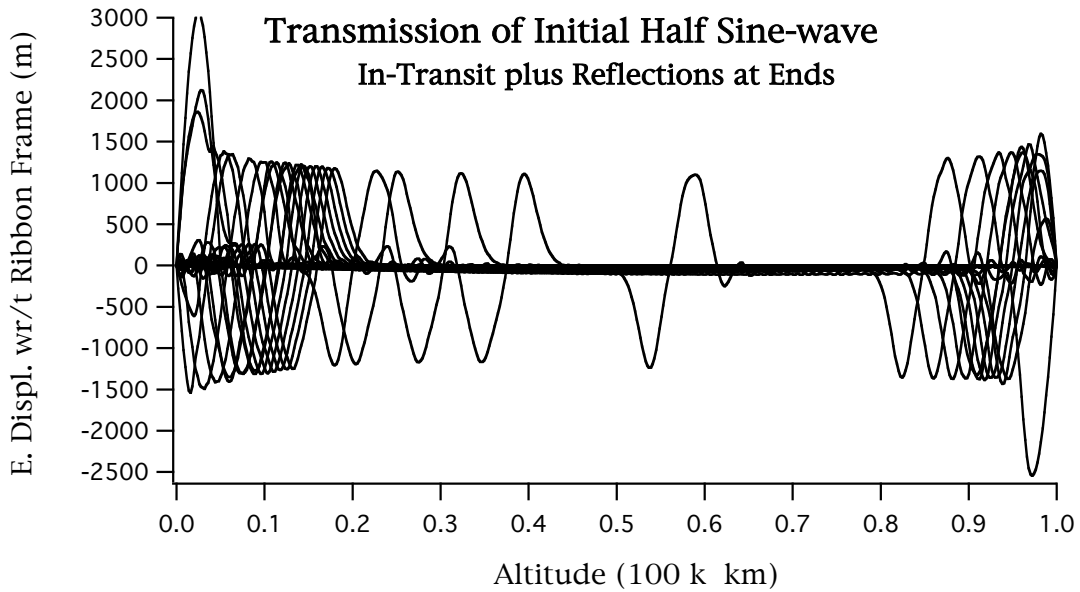


The two graphs indicate that only insignificant coupling (at best) is occurring. Below, is the time history of the mid-point of the ribbon. These are displacements relative to the line between the anchor and the ballast. The dotted line is the “in-plane” response. Again nothing indicates significant coupling between these modes. Note the difference in the natural frequencies of the two modes and, also the fact that the in-plane response is showing small component of in-plane pendulus libration coupling; this libration is an artifact of the simulation (imperfect) initialization rather than having been precipitated by the 1st string mode activity.

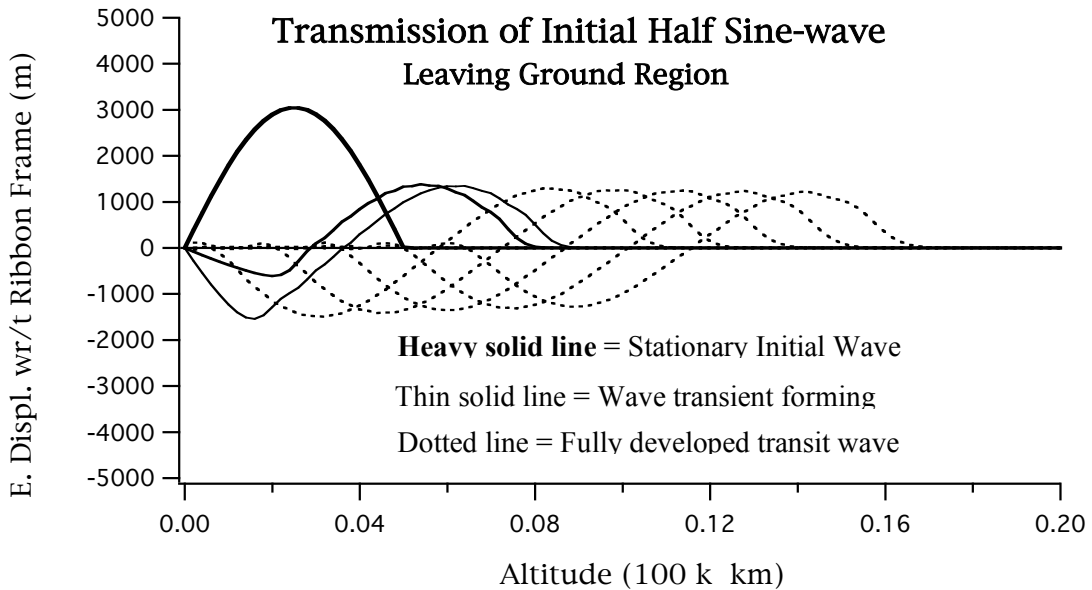


2.3.4 Transverse Wave Propagation

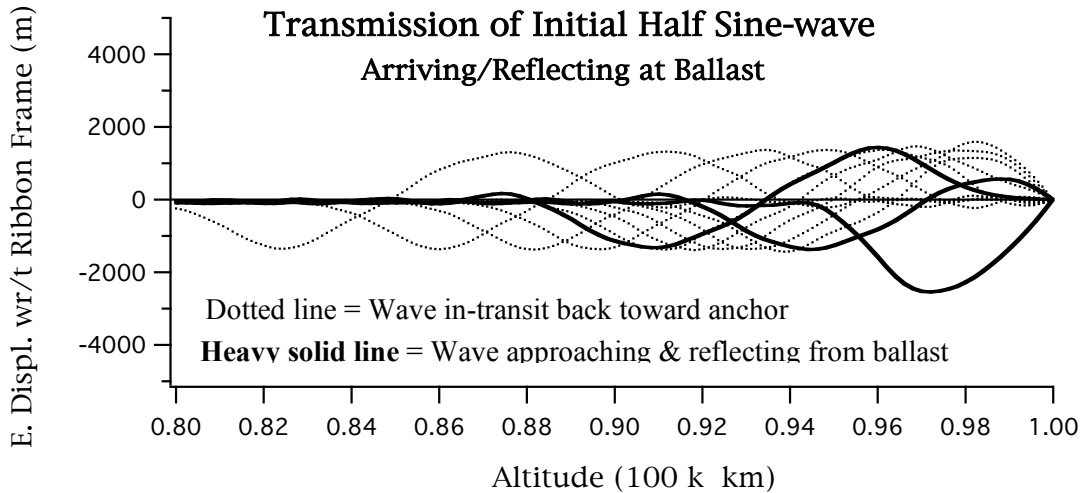
Transverse wave propagation is shown for the elevator ribbon. The wave is In-Plane, and is created as an initial condition at the ground consisting of a transverse deflection in the shape of a stationary 3000 m displacement half-sine wave extending over 5% of the ribbon length. It propagates the length of the ribbon, reflects off the ballast, returns to the anchor, at which it again reflects back upwards towards the ballast. The graph below shows many snapshots of the waves states as it progresses back and forth along the length.



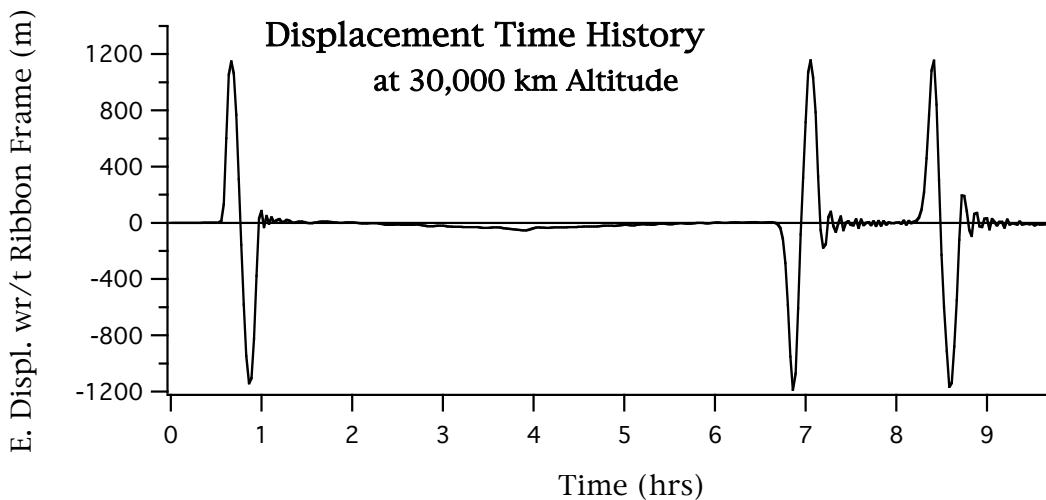
Below shows the initial wave leaving the ground and starting the trip towards the ballast.



The graph below shows the wave arriving at, then reflecting from the ballast end. Note that the wave has suffered some shape distortion due to the realities of the actual ribbon properties deviating from that which would predicate a classical (ie. un-distorted) wave propagation.



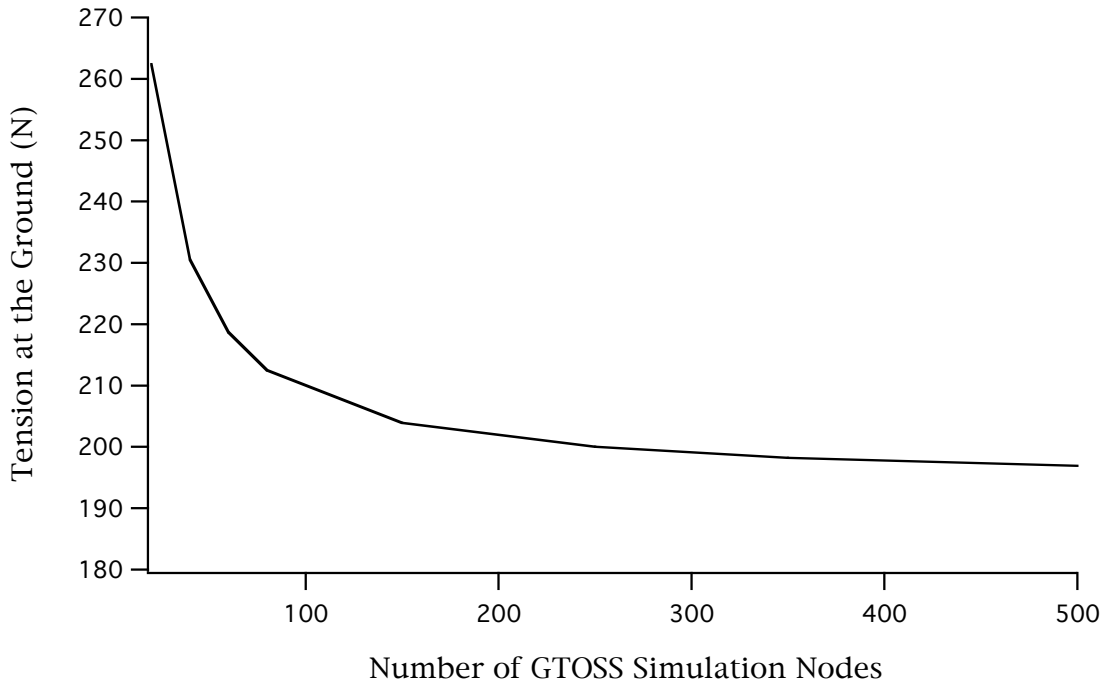
The graph below shows a displacement time-history at an altitude of 30,000 km. The initial pulse (at about 3/4 hours) represents the wave's first appearance at that altitude after it leave the ground. The wave must then make a trip from that point of 70,000 km, to reach and reflect off the ballast; it then makes the same trip back down before reappearing at 30,000 km altitude (the second pulse at about 7 hours). The same scenario ensue except this time it is the ground (only 30,000 k km away), that it travels to, reflects then again makes its appearance at 30,000 k km.



Notice also that the wave shape progressively deteriorates in time due to actual ribbon properties, reflections (and to some degree the numerical simulation process producing these results).

2.4 GRAVITY-WELL SIMULATION CONVERGENCE

To properly simulate a space elevator configuration using a discrete nodal approach, one must pay attention to the spatial-convergence of the simulation as it pertains to the “gravity well” (ie. inverse-square planetary gravity model). The graph below depicts (for the Earth) the tension at the anchor point as a function of the number of “uniformly-spaced” nodes used to simulate the elevator ribbon.



It can be seen that for node-counts greater than 200, the earth’s gravity-well is being fairly well acknowledged. For lesser node counts, simulation results may still be acceptable, depending upon the degree to which total-available anchor tension must be fully realized.

Note also, that *non-uniform* distributions of lesser node-counts (for instance 100 nodes from ground to 10,000 km, then 50 nodes between there and ballast, etc) may suffice to fully acknowledge the gravity well.